Photoionization of two-shell endohedral atoms

M. Ya. Amusia,[1,2] L. V. Chernysheva,[1] and E. Z. Liverts[2]

[1]*A. F. Ioffe Physical-Technical Institute, 194021 St. Petersburg, Russia*
[2]*Racah Institute of Physics, Hebrew University, 91904 Jerusalem, Israel*
(Received 5 May 2009; published 4 September 2009)

The photoionization of a two-shell endohedral $A @ C_{N1} @ C_{N2}$ is considered. Formulas are presented for cross sections and angular anisotropy parameters, both dipole and nondipole. The effect of the fullerenes shell upon photoelectron from atom A is taken into account substituting the action of the fullerene by two zero-thickness "bubble potential." The fullerenes shells polarization is included assuming that the radius of the outer shell R_2 is much bigger than the inner R_1 and both much exceed the atomic radius r. This permits to express the effect via $C_{N1,N2}$ polarizabilities, which are connected to their photoionization cross sections. The interaction between shells C_{N1} and C_{N2} is taken into account in the random phase approximation (RPA). The effect of photoelectron scattering by both "bubble potentials" is included in the lowest order and in the RPA frame. As concrete examples, two endohedrals $Ar @ C_{60} @ C_{240}$ and $Xe @ C_{60} @ C_{240}$ are considered. In the $Ar @ C_{60} @ C_{240}$ case we consider $3p$ and $3s$, while in the case $Xe @ C_{60} @ C_{240}$ $5p$, $5s$ and $4d$ subshells are considered. A whole variety of peculiarities are found that deserve experimental verification.

I. INTRODUCTION

A lot of attention is given in recent years to photoionization of endohedral atoms [1–4]. These are objects consisting of a fullerene C_N and an atom A, inserted inside, $A @ C_N$. The attention is concentrated on the modification of this atom photoionization characteristic. Indeed, the difference of them as compared to that of isolated atom A gives information on the fullerenes structure. In a sense, the inner atom A in $A @ C_N$ serves as a "lamp" that shines "light" in the form of photoelectron waves that "illuminates" the fullerene C_N from the inside.

A number of specific features were predicted in photoionization of $A @ C_N$ that makes it different from photoionization of an isolated atom A itself. Most prominent features are the so-called confinement [5] and Giant endohedral [6] resonances that are consequences of two prominent effects—the reflection of the photoelectrons by the fullerenes shell and modification of the incoming photon beam due to C_N polarization [7,8]. In spite of considerable theoretical efforts, there are quite a few experimental investigations in this area [9,10].

What is easier to calculate is more difficult to measure and vice versa. As an object of calculations the almost ideally spherically symmetric fullerene C_{60} is usually considered, while experiment is done for deformed C_{80} and C_{82}. As inner atoms noble gases, hydrogen and alkali atoms are main objects of calculations, whereas in experiments Ce, Pr, and their ions are considered. We do believe, however, that this process of mutual attempts will converge in not too distant future, demonstrating whether the developed calculation approaches are accurate enough.

Meanwhile, it appeared that fullerenes could be two-shell structures [11,12]. It seems, therefore, timely to consider an endohedral of such type that we denote as $A @ C_{N1} @ C_{N2}$. In this paper we will study such an object using to describe reflection a rather simple approach that substitute both shells by infinitely thin potential layers. We will call it two-bubble potential. How to take into account a single bubble potential is described at length in e.g., [13]. Here we will present formulas for the two-bubble potential. We will assume that since the radius of the outer bubble is considerably bigger than the inner one, they are not affecting each other. This is why for experimentally known radiuses R_1, R_2 and corresponding number of carbon atoms in it, N_1, N_2, respectively, we obtain the potential strength of both of them V_1, V_2, using experimentally known electron affinities I_1, I_2 of fullerenes C_{N1} and C_{N2}, just as it was done for an ordinary bubble potential [13].

As it was already mentioned in a number of places (e.g., [14]), the "bubble" (or, more solemnly, "orange skin") potential is valid when the photoelectron's wavelength is much bigger than the fullerenes thickness. In numbers, it means photoelectron's energy up to 2–3 Ry. As a concrete example, we will consider two shells, with $N_1 = 60$ and $N_2 = 240$

Assuming that the fullerenes radius is much bigger than the atomic one, the effect of fullerenes polarization upon the incoming photon beam can be expressed via fullerenes polarizability [7]. The latter via dispersion relation is connected to the experimentally measurable fullerenes photoionization cross section [15]. We will assume for simplicity that the outer fullerenes radius is much bigger than the inners one. In this approximation we will take into account not only the fullerenes action upon the atom's photoionization, but mutual influence of both fullerenes shells as well. Since the photoionization cross section of C_{240} is unknown, we will use rather approximate scaling to estimate the polarizability of this object.

II. PHOTOELECTRON SCATTERING BY TWO-BUBBLE POTENTIAL

The two-bubble potential is of the form

$$V(r) = -V_1\delta(r - R_1) - V_2\delta(r - R_2) \qquad (1)$$

so that the equation for a photoelectron with the angular momentum l and energy E moving in the atomic potential $U(r)$ is of the form[1]

$$\frac{1}{2}\left[\chi''_{kl} - \frac{l(l+1)}{r^2}\chi_{kl}\right] + [V_1\delta(r - R_1) + V_2\delta(r - R_2) - U(r)$$
$$+ E]\chi_{kl} = 0, \qquad (2)$$

and has solutions:

$$\chi_{kl}(r) = \begin{cases} F_l(k)u_{kl}(r) & (r \leq R_1) \\ C_1 u_{kl}(r) + C_2 v_{kl}(r) & (R_1 < r \leq R_2) \\ u_{kl}(r)\cos\delta_l - v_{kl}(r)\sin\delta_l & (R_2 < r). \end{cases} \qquad (3)$$

Here $k = \sqrt{2E}$.

Let us introduce the following notations:

$$F_l(k) \equiv F,$$

$$u_{kl}(R_1) \equiv u_1,$$

$$u_{kl}(R_2) \equiv u_2,$$

$$v_{kl}(R_1) \equiv v_1,$$

$$v_{kl}(R_2) \equiv v_2. \qquad (4)$$

Then the condition of the wave function continuity (4) at $r = R_1$ acquires the form

$$Fu_1 = C_1 u_1 + C_2 v_1. \qquad (5)$$

Integration of Eq. (2) near the point $r = R_1$ gives

$$Fu'_1 = C_1 u'_1 + C_2 v'_1 + 2V_1 Fu_1. \qquad (6)$$

Multiplying Eqs. (5) and (6) by u'_1 and u_1, respectively, and then subtracting one equation from another, the following relation is obtained

$$C_2(u_1 v'_1 - v_1 u'_1) = -2V_1 Fu_1^2. \qquad (7)$$

By inserting here the so-called Wronskian relation

$$u_{kl}(r)v'_{kl}(r) - v_{kl}(r)u'_{kl}(r) = k, \qquad (8)$$

it is obtained,

$$C_2 k = -2V_1 Fu_1^2. \qquad (9)$$

Excluding F from Eqs. (5) and (9), the first equation,

connecting the coefficients C_1 and C_2 is obtained,

$$2V_1 u_1^2 C_1 = -(k + 2V_1 u_1 v_1)C_2. \qquad (10)$$

Let us consider now the point $r = R_2$ from the outside of the spherical layer. From the continuity conditions for the wave function (3) at this point, one obtains

$$(C_1 u_2 + C_2 v_2) = u_2 \cos\delta_l - v_2 \sin\delta_l. \qquad (11)$$

Integration of Eq. (2) near $r = R_2$ gives

$$-2V_2(C_1 u_2 + C_2 v_2) = u'_2 \cos\delta_l - v'_2 \sin\delta_l - C_1 u'_2 - C_2 v'_2. \qquad (12)$$

Multiplying Eqs. (11) and (12) by u'_2 and u_2, respectively, and then subtracting the first equation from the second one, the following relation is obtained

$$\sin\delta_l = -C_2 + \frac{2V_2 u_2(C_1 u_2 + C_2 v_2)}{k}. \qquad (13)$$

If one multiplies Eqs. (11) and (12) instead by v'_2 and v_2, respectively, and then subtracts the first equation from the second one, another relation is obtained,

$$\cos\delta_l = C_1 + \frac{2V_2 v_2(C_1 u_2 + C_2 v_2)}{k}. \qquad (14)$$

In the derivation of Eqs. (13) and (14), we used the Eq. (8).

Using the well-known relations for the trigonometric functions, the second relation, connecting the coefficients C_1 and C_2 is obtained,

$$[kC_1 + 2V_2 v_2(C_1 u_2 + C_2 v_2)]^2 + [kC_2 - 2V_2 u_2(C_1 u_2 + C_2 v_2)]^2 = k^2. \qquad (15)$$

At last, solving the system of Eqs. (10) and (15) for coefficients C_1 and C_2 we obtain

$$C_1 = \frac{k(k + 2V_1 u_1 v_1)}{\sqrt{\zeta}}, \quad C_2 = -\frac{2kV_1 u_1^2}{\sqrt{\zeta}}, \qquad (16)$$

where

$$\zeta = k^4 + 4k^3(V_1 u_1 v_1 + V_2 u_2 v_2) + 16V_1^2 V_2^2 u_1^2 (u_2 v_1 - u_1 v_2)^2 (u_2^2 + v_2^2) - 16kV_1 V_2 u_1(u_1 v_2 - u_2 v_1)[V_1 u_1(u_1 u_2 + v_1 v_2) + V_2 u_2(u_2^2 + v_2^2)] + 4k^2\{V_1^2 u_1^2(u_1^2 + v_1^2) + V_2^2 u_2^2(u_2^2 + v_2^2) + 2V_1 V_2 u_1[2u_2 v_1 v_2 + v_1(u_2^2 - v_2^2)]\}. \qquad (17)$$

Inserting expressions (16) for C_1 and C_2 into (13), we obtain

---

[1]We employ the atomic system of units with electron charge e, mass m, and Plank constant equal to 1, $e = m = \hbar = 1$.

$$\sin \delta_l = \frac{2}{\sqrt{\zeta}}\{kV_2u_2^2 + V_1u_1[ku_1 + 2V_2u_2(u_2v_1 - u_1v_2)]\}.$$

(18)

Removing the coefficient C_2 from Eqs. (9) and (16), the following simple relations for the *reflection amplitude F* and phase δ_l are obtained:

$$F \equiv F_l(k) = \frac{k^2}{\sqrt{\zeta}}$$

$$= \frac{k \sin \delta_l}{2[V_1u_1^2 + V_2u_2^2 - 2V_1V_2u_1u_2(u_1v_2 - u_2v_1)/k]},$$

$$\tan \delta_l(k)$$

$$= \frac{u_1^2 + u_2V_2[u_2/V_1 + 2u_1V_1(u_2v_1 - u_1v_2)/k]}{u_1v_1 + k/2V_1 + u_2v_2V_2/V_1 - 2u_1v_2V_2(u_2v_1 - u_1v_2)/k}.$$

(19)

It is easy to verify that by putting $R_1 = R_2$ in Eqs. (13), (14), (17), and (19), the following relations follow:

$$F_l(k) = \frac{k \sin \delta_l}{2V_0u_{kl}^2(R)},$$

$$\tan \delta_l = \frac{u_{kl}^2(R)}{u_{kl}(R)v_{kl}(R) + k/2V_0}, \qquad (20)$$

that coincides with corresponding relations for single-wall fullerene with $R_2 \rightarrow R$ and $(V_1 + V_2) \rightarrow V_0$ (see, e.g., [16]).

III. POLARIZATION EFFECTS FROM THE TWO-SHELL FULLERENE

As it was already demonstrated quite a while ago, the following relation can account for the polarization of the fullerene under the action of the incoming photon beam [7]:
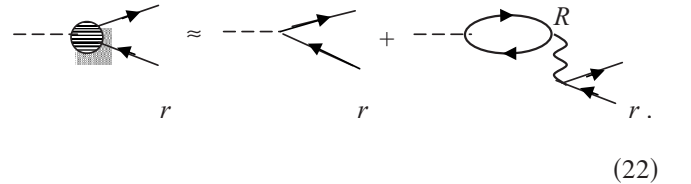
$$D_{AC}(\omega) \cong D_A(\omega)\left[1 - \frac{\alpha(\omega)}{R^3}\right], \qquad (21)$$

where $D_{AC}(\omega)$ is the endohedral atom $A @ C_N$ photoionization dipole amplitude, $D_A(\omega)$ is the same for an isolated atom, $\alpha(\omega)$ is the fullerenes dipole polarizability, R is its radius. This relation is derived under valid assumption that R is much bigger than the atomic radius r_A.

It is convenient to represent the interaction of an incoming photon with an atom A inserted inside a two-shell fullerene using diagrammatical approach, represented in the form suitable for atomic physics in, e.g., [17]. The standard notations are used in the diagrams below: a horizontal dashed line stands for an incoming photon, vertically oriented wavy line represent the Coulomb interelectron interaction, solid line with an arrow to the right (left) stands for electron (vacancy), respectively. The shadowed circle denotes the total amplitude of atom A photoionization with participation of both fullerenes shell.

The simplest way to take into account the fullerenes polarization is to consider the photoionization of $A @ C_N$ in the frame of the random phase approximation with exchange (RPAE) that proved to be very successful in describing photoionization of multielectron atoms [18]. If the atomic radius r_A is much smaller than $R, R \gg r$, the photoionization amplitude $D_{AC}(\omega)$ of the atom A caged inside fullerene C_N can be represented diagrammatically as [7]

(22)

The first term in Eq. (22) represents the pure atomic photoionization amplitude while the second is a contribution to ionization of atom A via virtual excitations of the fullerenes shell. If $R \gg r$, Eq. (22) permits to go well beyond the lowest order term in interelectron interaction by assuming that correlations between separately atomic and fullerenes electrons in RPAE or even out of its frame are included in the amplitude $D_A(\omega)$ and the fullerenes electron-vacancy loop. It can be demonstrated that higher order terms in atom-fullerene interaction is suppressed by the factor $\alpha^A(\omega)/R^3 \ll 1$, where $\alpha^A(\omega)$ is the A atom dipole polarizability.

For two-shell fullerene the corresponding expression is much more complex, since in principal the interaction between two group of electrons, belonging to fullerenes 1 and 2 must be taken into account. Under a reasonable qualitatively correct assumption, that holds at least for considered in this paper C_{60} and C_{240}, the following relation is correct $r \ll R_1 \ll R_2$. In this case the amplitude $D_{AC}(\omega)$ is presented by the infinite sequence of the following diagrams:

$$(23)$$

For simplicity of the drawings we have omitted so-called time-reverse diagrams.

The inequalities $r \ll R_1 \ll R_2$ permit to simplify the interactions between atomic and fullerene 1 and 2 electrons considerably, presenting it as $\vec{r}\vec{R}_1/R_1^2$, $\vec{r}\vec{R}_2/R_2^2$, and $\vec{R}_1\vec{R}_2/R_2^2$, respectively. The sequence can be summed, leading to appearance of the same denominator den to the contributions of all first and second order terms in the rhs of Eq. (23),

$$\text{den} = 1 - \frac{\alpha_1 \alpha_2}{R_2^6}, \tag{24}$$

where $\alpha_1 \equiv \alpha_1(\omega)$, $\alpha_2 \equiv \alpha_2(\omega)$, R_1, and R_2 are the dipole polarizability and radiuses of the fullerenes 1 and 2, respectively. Finally, we arrive for $D_{AC}(\omega)$ to the following expression:

$$
\begin{aligned}
&D_{AC}(\omega) \\
&\cong D_A(\omega)\left[1 - \left(\frac{\alpha_1}{R_1^3} + \frac{\alpha_2}{R_2^3}\right) \frac{1 - \dfrac{\alpha_1 \alpha_2}{\alpha_1 R_2^3 + \alpha_2 R_1^3}\left(1 + \dfrac{R_1^3}{R_2^3}\right)}{1 - \dfrac{\alpha_1 \alpha_2}{R_2^6}} \right] \\
&\equiv G_{12}(\omega) D_A(\omega),
\end{aligned}
\tag{25}
$$

where $G_{12}(\omega)$ is the *polarization amplitude factor* for two-shell fullerene.

It is seen that the correction due to simultaneous polarization of both fullerenes shells proportional to $\alpha_1 \alpha_2$ considerably modifies a simple formula that would account only for the sum of the shells action.

It is essential to have in mind that Eq. (25) can in principle take into account electron correlations beyond the RPAE frame. Namely, each of the polarizabilities, α_1 or α_2, can include even *all* correlations inside each fullerene, 1 or 2, respectively. It means that as polarizabilities, accurately calculated or experimentally measured can be used.

IV. DETERMINATION OF POLARIZABILITIES

Polarizabilities α_1 and α_2 can be calculated or taken from experiment. Directly determined in experiment are only static polarizabilities, namely their values at $\omega \approx 0$. To obtain dynamic polarizability, calculations are needed. However, if photoionization cross section $\sigma(\omega)$ of a considered object is measured, the dynamic polarizability can be derived using the following relations:

$$\text{Im } \alpha(\omega) = c \frac{\sigma(\omega)}{4\pi\omega},$$

$$\text{Re } \alpha(\omega) = \frac{c}{2\pi^2} \int_I^\infty \frac{\sigma(\omega')d\omega'}{\omega'^2 - \omega^2}, \tag{26}$$

where c is the speed of light and I is the fullerenes ionization potential. Note that in the second relation in Eq. (26), the so-called dispersion relation, it is assumed that the contribution of discrete excitations can be neglected. That is indeed confirmed by existing experimental data on fullerenes photoionization [19].

The results for polarizability obtained using Eq. (26) have to satisfy two constrains. The first is the static polarizability value that can be measured independently and has in principal to coincide with the following value:

$$\alpha(0) = \frac{c}{2\pi^2} \int_I^\infty \frac{\sigma(\omega)d\omega}{\omega^2}. \tag{27}$$

The second constrain comes from the opposite limit of high frequencies of radiation $\omega \to \infty$, where by using the dipole sum rule the following relation is obtained:

$$\text{Re } \alpha_d(\omega \to \infty) = -\frac{1}{\omega^2} \frac{c}{2\pi^2} \int_I^\infty \sigma(\omega')d\omega' = -\frac{N}{\omega^2}, \tag{28}$$

where N is the total number of electrons in the considered fullerene. In fullerenes each atom gives up four of its electrons to the fullerene electron shell while the remaining two stay close to the nucleus. The inner electrons ionization threshold I_{in} is much higher than I. The cross section is concentrated near I. As a result the integral in Eq. (28) is saturated well below I_{in}. Therefore N is four times the number of atoms in C_{N_n}, $N = 4N_n$.

In principal, not absolute but relative experimental data on $\sigma(\omega)$ are sufficient. This is because the relative values can be putted on the absolute scale using the sum rule,

$$(c/2\pi^2) \int_{I_o}^\infty \sigma(\omega)d\omega = N, \tag{29}$$

While the experimental data on $\sigma(\omega)$ for C_{60} are known, and $\alpha(\omega)$ can be reliably derived, this is not the case for C_{240}. Therefore we will use a simple estimate scaling to obtain $\alpha(\omega)$ for this object (see below).

V. DERIVATION OF PARAMETERS

To perform photoionization calculations we need to know the fullerenes potentials V_1 and V_2 that enter the Eq. (2). They can be determined using for each of the shells the same formula that is usually employed for a single-shell fullerene [13], so that

$$V_{1,2} = \frac{1}{2}\sqrt{2I_{1,2}}(1 + \coth\sqrt{2I_{1,2}}R_{1,2}), \tag{30}$$

where $I_{1,2}$ are the electron affinities of the fullerenes with N_1 and N_2 carbon atoms, respectively. By doing this we make a reasonable assumption that well separated shells are not essentially affecting each other so that a two-shell "onion" C_{N_1,N_2} really consists of two fullerenes C_{N_1} and C_{N_2}. As a concrete example we consider in this paper fullerenes with $N_1 = 60$ and $N_2 = 240$. The electron affinities I_1 and I_2 for C_{60} and C_{240} taken from [20] are the following: $I_{60} = 0.0974$ and $I_{240} = 0.140$. For completeness let us add $I_{540} = 0.386$. The radiuses of these fullerenes are also known, being equal to

$R_{60} \cong 6.72$, $R_{240} \cong 13.5$, and $R_{540} \cong 19.8$.[2] It is remarkable that at least for considered objects the ratios $\eta_n \equiv N_n/R_n^2$ are almost the same $\eta_{60} = 1.317$, $\eta_{240} = 1.317$, $\eta_{540} = 1.38$. So, let us assume for η_n a universal value 1.32.

Analysis of the C_{60} polarizability permitted to conclude that at least for static values $\alpha_{C60} \approx 60\alpha_C$, where α_C is the static polarizability of a single carbon atom. Since the density of generalized electrons for all big enough fullerenes is the same, the position of the giant resonance that dominates their photoionization cross sections coincides, just as the shape of the photoionization cross sections. Having this and Eq. (29) in mind, it is natural to assume that equation $\alpha_{C_n}(\omega) \cong N_n\alpha_C(\omega)$ holds for all considered fullerenes and at any ω. So, not only in the static limit the relation $\alpha_{C_n} \approx N_n\alpha_C$ is valid.

In order to estimate the contribution of the second fullerenes shell, let us use of this relation. Using the ratio $\eta_n = 1.32$ and these assumptions, we obtain $\alpha_{N_n}(\omega)/R_n \approx \alpha_{C_{60}}(\omega)/45.5R_n \equiv \alpha_1(\omega)/45.5R_n$. With the help of this relation we derive from Eq. (25)

$$D_{AC}(\omega) \approx D_A(\omega)\left[1 - 1.51\frac{\alpha_1}{R_1^3}\frac{1 - 0.380\alpha_1(\omega)}{1 - 0.0635[\alpha_1(\omega)/R_1^3]^2}\right]$$

$$\equiv G_{12}^a(\omega)D_A(\omega), \tag{31}$$

where $G_{12}^a(\omega)$ is the approximate value of the polarization amplitude factor. The data of $\alpha_1(\omega)$ as well as of $S_1(\omega) = |(1 - \alpha_1(\omega)/R_1^3)|^2$ are taken from [15].

VI. FORMULAS FOR CALCULATIONS

In this section we will present the formulas required to calculate the photoionization cross sections and angular anisotropy parameters, both dipole and nondipole for two-shell endohedral atom $A @ C_{N_1} @ C_{N_2}$.

Let us start with the case, when the effects of fullerenes shells potential action upon photoelectrons of atom A is sufficient to take into account perturbative. Then the following relation connects pure atomic partial photoionization cross-section $\sigma_{nl,kl'}^A(\omega)$ ($l' = l \pm 1$) for the transition $nl \to kl'$ to the corresponding partial cross-section of the endohedral $A @ C_{N_1} @ C_{N_2}$

$$\sigma_{nl,kl'}^{AC_{12}}(\omega) = |F_{l'}(k)|^2 S_{12}(\omega)\sigma_{nl,kl'}^A(\omega), \tag{32}$$

which is similar to that of the one-shell endohedral [14]. Here $S_{12}(\omega) = |G_{12}(\omega)|^2$ is the *polarization factor*. The relation (32) presents the photoionization cross section of an endohedral in a separable form, as a product of atomic cross-section, reflection, and polarization factors.

The total photoionization cross-section is obtained from Eq. (32) by summing over l',

---

[2]All the values of electron affinity and radiuses are in atomic units that will be used throughout all this paper.

$$\sigma_{nl}^{AC_{12}}(\omega) = \sum_{l'=l\pm1} \sigma_{nl,kl'}^{AC_{12}}(\omega). \tag{33}$$

The differential in angle $d\Omega$ cross section of the photo-electron's emission under the action of nonpolarized light is given for spherically symmetric fullerenes shell, having the same center, by the following expression:

$$\frac{d\sigma_{nl}^{AC_{12}}(\omega)}{d\Omega} = \frac{\sigma_{nl}^{AC_{12}}(\omega)}{4\pi}\left[1 - \frac{1}{2}\beta_{nl}(\omega)P_2(\cos\theta)\right.$$
$$\left. + \kappa\gamma_{nl}(\omega)P_1(\cos\theta) + \kappa\eta_{nl}(\omega)P_3(\cos\theta)\right]. \tag{34}$$

Here $\kappa = \omega/c$, c is the speed of light and $P_i(\cos\theta)$ are the Legendre polynomials.

The dipole angular anisotropy parameter $\beta_{nl}(\omega)$ is not affected by the fullerenes shell polarization amplitude and is given by

$$\beta_{nl}(\omega) = \frac{1}{(2l+1)[(l+1)F_{l+1}^2\widetilde{D}_{l+1}^2 + lF_{l-1}^2\widetilde{D}_{l-1}^2]}[(l+1)$$
$$\times(l+2)F_{l+1}^2\widetilde{D}_{l+1}^2 + l(l-1)F_{l-1}^2\widetilde{D}_{l-1}^2 - 6l(l$$
$$+1)F_{l+1}F_{l-1}\widetilde{D}_{l+1}\widetilde{D}_{l-1}\cos(\widetilde{\delta}_{l+1} - \widetilde{\delta}_{l-1})]. \tag{35}$$

Here dipole photoionization amplitudes $D_{l\pm1}(\omega)$ are complex numbers with module $\widetilde{D}_{l\pm1}(\omega)$, their phases being determined by relation $D_{l\pm1}(\omega) \equiv \widetilde{D}_{l\pm1}(\omega)\exp[i\Delta_{l\pm1}(k)]$. Relation $\widetilde{\delta}_{l'} = \delta_{l'} + \Delta_{l'}$ determined the phases $\widetilde{\delta}_{l'}$. Here and below F_{ν_i} are the reflection factors, given by Eq. (19) with ν_i determined by photoelectron's linear momentum $k_{\nu_i} = \sqrt{2\varepsilon_{\nu_i}}$ and l_{ν_i}. The corrections $G_{12}(\omega)$ are not entering $\beta_{nl}(\omega)$, since they are modifying the nominator and denominator in Eq. (35) similarly.

The situation with the nondipole angular anisotropy parameters that are given by the expressions derived in [18] is different, since they include corrections due to both dipole and quadrupole polarization amplitude $G_{12}^d(\omega)$ and $G_{12}^q(\omega)$,

$$\gamma_{nl}^{AC}(\omega) = \frac{3\widetilde{G}_{12}^q(\omega)}{5\widetilde{G}_{12}^d(\omega)[(l+1)F_{l+1}^2\widetilde{D}_{l+1}^2 + lF_{l-1}^2\widetilde{D}_{l-1}^2]} \times \left\{\frac{(l+1)F_{l+1}}{2l+3}[3(l+2)F_{l+2}\widetilde{Q}_{l+2}\widetilde{D}_{l+1}\cos(\widetilde{\widetilde{\delta}}_{l+2} - \widetilde{\widetilde{\delta}}_{l+1}) - lF_l\widetilde{Q}_l\widetilde{D}_{l+1}\cos(\widetilde{\widetilde{\delta}}_{l+2}\right.$$
$$\left. - \widetilde{\widetilde{\delta}}_{l+1})] - \frac{lF_{l-1}}{2l+1}[3(l-1)F_{l-2}\widetilde{Q}_{l-2}\widetilde{D}_{l-1}\cos(\widetilde{\widetilde{\delta}}_{l-2} - \widetilde{\widetilde{\delta}}_{l-1}) - (l+1)F_l\widetilde{Q}_l\widetilde{D}_{l-1}\cos(\widetilde{\widetilde{\delta}}_l - \widetilde{\widetilde{\delta}}_{l-1})]\right\}, \tag{36}$$

$$\eta_{nl}^{AC}(\omega) = \frac{3\widetilde{G}_{12}^q(\omega)}{5\widetilde{G}_{12}^d(\omega)[(l+1)F_{l+1}^2\widetilde{D}_{l+1}^2 + lF_{l-1}^2\widetilde{D}_{l-1}^2]} \times \left\{\frac{(l+1)(l+2)}{(2l+1)(2l+3)}F_{l+2}\widetilde{Q}_{l+2}[5lF_{l-1}\widetilde{D}_{l-1}\widetilde{D}_{l-1}\cos(\widetilde{\widetilde{\delta}}_{l+2} - \widetilde{\widetilde{\delta}}_{l-1})\right.$$
$$- (l+3)F_{l+1}\widetilde{D}_{l+1}\cos(\widetilde{\widetilde{\delta}}_{l+2} - \widetilde{\widetilde{\delta}}_{l-1})] - \frac{(l-1)l}{(2l+1)(2l+1)}F_{l-2}\widetilde{Q}_{l-2} \times [5(l+1)F_{l+1}\widetilde{D}_{l+1}\cos(\widetilde{\widetilde{\delta}}_{l-2} - \widetilde{\widetilde{\delta}}_{l+1})$$
$$- (l-2)F_{l-1}\widetilde{D}_{l-1}\cos(\widetilde{\widetilde{\delta}}_{l-2} - \widetilde{\widetilde{\delta}}_{l-1})] + 2\frac{l(l+1)F_l\widetilde{Q}_l}{(2l-1)(2l+3)}[(l+2)F_{l+1}\widetilde{D}_{l+1}\widetilde{D}_{l+1}\cos(\widetilde{\widetilde{\delta}}_l - \widetilde{\widetilde{\delta}}_{l+1}) - (l-1)F_{l-1}\widetilde{D}_{l-1}\widetilde{D}_{l-1}\cos(\widetilde{\widetilde{\delta}}_l$$
$$- \widetilde{\widetilde{\delta}}_{l-1})]\right\}. \tag{37}$$

They include also quadrupole photoionization matrix elements $Q_{l,l\pm2}$ that, being complex numbers can be presented as $Q_{l,l\pm2}(\omega) \equiv \widetilde{Q}_{l,l\pm2}(\omega)\exp[i\Delta_{l,l\pm2}(k)]$, where $\widetilde{Q}_{l,l\pm2}(\omega)$ is the module of $Q_{l,l\pm2}(\omega)$ [21].

Very often experimentalists are using nondipole parameters γ_{nl}^C and δ_{nl}^C, introduced in [22,23]. The following for-mula connect them to those defined by Eqs. (36) and (37),

$$\gamma_{nl}^C/5 + \delta_{nl}^C = \kappa\gamma_{nl}, \quad \gamma_{nl}^C/5 = -\kappa\eta. \tag{38}$$

The dipole polarization amplitude factor is determined by Eq. (25), while the quadrupole one is given by similar to Eq. (25) relation

$$Q_{AC}(\omega) \cong Q_A(\omega) \left[1 - \left(\frac{\alpha_1^q}{4R_1^5} \right. \right.$$

$$\left. \left. + \frac{\alpha_2^q}{4R_2^5} \frac{1 - \frac{\alpha_1^q \alpha_2^q}{4\alpha_1^q R_2^5 + 4\alpha_2^q R_1^5} \left(1 + \frac{R_1^5}{R_2^5} \right)}{1 - \frac{\alpha_1^q \alpha_2^q}{16R_2^6}} \right) \right]$$

$$\equiv G_{12}^q(\omega) Q_A(\omega), \qquad (39)$$

where α_1^q and α_2^q are the dynamic quadrupole polarizabilities of the inner and outer fullerene, respectively. Note, that for a single-wall fullerene the quadrupole polarization amplitude factor is given by the relation [18]

$$Q_{AC}(\omega) \cong Q_A(\omega) \left(1 - \frac{\alpha_q(\omega)}{4R^5} \right) \equiv Q_A(\omega) G^q(\omega), \quad (40)$$

Being complex numbers, the polarization amplitude factors $G_{12}^{q,d}(\omega)$ can be presented as

$$G_{12}^{q,d}(\omega) = \widetilde{G}_{12}^{q,d}(\omega) \exp[i\Lambda^{q,d}(\omega)], \qquad (41)$$

where $\widetilde{G}_{12}^{q,d}(\omega)$ are the module of $G_{12}^{q,d}(\omega)$.

In Eqs. (36) and (37) the following notations for phases are used $\widetilde{\widetilde{\delta}}_{l\pm1} = \widetilde{\delta}_{l\pm1} + \Lambda^d = \delta_{l\pm1} + \Delta_{l\pm1} + \Lambda^d$ and $\widetilde{\widetilde{\delta}}_{l\pm2,l} = \widetilde{\delta}_{l\pm2,l} + \Lambda^q = \delta_{l\pm2,l} + \Delta_{l\pm2,l} + \Lambda^q$.

If the reflection of photoelectrons by the fullerene shell is strong, it is insufficient to take it into account in the lowest order in $F_{l'}(k)$ as was done in Eq. (32). Natural is to take multiple reflection within the RPAE frame that is achieved by solving the following equation for the dipole amplitude:

$$\langle \nu_1 | \breve{D}(\omega) | \nu_2 \rangle = \langle \nu_1 | \hat{d} | \nu_2 \rangle + \sum_{\nu_3, \nu_4} \frac{\langle \nu_3 | \breve{D}(\omega) | \nu_4 \rangle [F_{\nu_3}^2 n_{\nu_4}(1 - n_{\nu_3}) - F_{\nu_4}^2 n_{\nu_3}(1 - n_{\nu_4})] \langle \nu_4 \nu_1 | U | \nu_3 \nu_2 \rangle}{\varepsilon_{\nu_4} - \varepsilon_{\nu_3} + \omega + i\eta(1 - 2n_{\nu_3})} \qquad (42)$$

and for the quadrupole amplitude

$$\langle \nu_1 | \breve{Q}(\omega) | \nu_2 \rangle = \langle \nu_1 | \hat{q} | \nu_2 \rangle + \sum_{\nu_3, \nu_4} \frac{\langle \nu_3 | \breve{Q}(\omega) | \nu_4 \rangle [F_{\nu_3}^2 n_{\nu_4}(1 - n_{\nu_3}) - F_{\nu_4}^2 n_{\nu_3}(1 - n_{\nu_4})] \langle \nu_4 \nu_1 | U | \nu_3 \nu_2 \rangle}{\varepsilon_{\nu_4} - \varepsilon_{\nu_3} + \omega + i\eta(1 - 2n_{\nu_3})}. \qquad (43)$$

Here $\langle \nu_i | d | \nu_j \rangle$ and $\langle \nu_i | q | \nu_j \rangle$ are the dipole and quadrupole photon-electron interaction matrix elements, respectively; n_ν is the Fermi step function: $n_\nu = 1$, if ν is an occupied level and $n_\nu = 0$ if ν is an empty one. It is implied that $\eta \to 0$ in Eqs. (42) and (43). The relations (42) and (43) generalize the RPAE equations for an atom surrounded by zero-thickness potential shell.

The relation (32) with pure atomic cross-section $\sigma_{nl,kl'}^A(\omega)$ is not valid any more. Instead, we have

$$\sigma_{nl,kl}^{AC_{12}}(\omega) = |F_{l'}(k)|^2 S_{12}(\omega) \widetilde{\sigma}_{nl,kl'}^A(\omega), \qquad (44)$$

where $\widetilde{\sigma}_{nl,kl'}^A(\omega)$ is given by the relation $\widetilde{\sigma}_{nl,kl'}^A(\omega) = \widetilde{\sigma}_{nl,kl'}^{A,\text{RPAE}}(\omega) |\breve{D}_{nl,kl'}(\omega)|^2 / |D_{nl,kl'}(\omega)|^2$ with $D_{nl,kl'}(\omega)$ being the photoionization amplitude of an isolated atom in RPAE, while $\breve{D}_{nl,kl'}(\omega)$ is given by Eq. (42). Instead of Eq. (35) we have

$$\beta_{nl}(\omega) = \frac{1}{(2l+1)[(l+1)F_{l+1}^2 \widetilde{D}_{l+1}^2 + lF_{l-1}^2 \widetilde{D}_{l-1}^2]} [(l+1)$$

$$\times (l+2)F_{l+1}^2 \widetilde{D}_{l+1}^2 + l(l-1)F_{l-1}^2 \widetilde{D}_{l-1}^2 - 6l(l$$

$$+1)F_{l+1}F_{l-1}\widetilde{D}_{l+1}\widetilde{D}_{l-1} \cos(\widetilde{\widetilde{\delta}}_{l+1} - \widetilde{\widetilde{\delta}}_{l-1})]. \qquad (45)$$

By substituting RPAE amplitudes $D_{l\pm1}$ and $Q_{l,l\pm2}$ with $\breve{D}_{l\pm1}(\omega) \equiv \widetilde{\widetilde{D}}_{l\pm1}(\omega) \exp[i\breve{\Delta}_{l\pm1}(k)]$ and $\breve{Q}_{l,l\pm2}(\omega) \equiv \widetilde{\widetilde{Q}}_{l,l\pm2}(\omega) \exp[i\breve{\Delta}_{l,l\pm2}(k)]$ from Eqs. (42) and (43) in Eqs. (36) and (37) or Eq. (38), we obtain nondipole angular anisotropy parameters with account of strong action of the fullerenes shell upon photoionization of two-shell endohedral atom. Note that corresponding phases $\widetilde{\widetilde{\delta}}_{l'}$ has to be substituted by $\widetilde{\widetilde{\delta}}_{l'}$ defined by the following relations $\widetilde{\widetilde{\delta}}_{l\pm1} = \widetilde{\delta}_{l\pm1} + \Lambda^d = \delta_{l\pm1} + \breve{\Delta}_{l\pm1} + \Lambda^d$ and $\widetilde{\widetilde{\delta}}_{l\pm2,l} = \widetilde{\delta}_{l\pm2,l} + \Lambda^q = \delta_{l\pm2,l} + \breve{\Delta}_{l\pm2,l} + \Lambda^q$ that take into account the difference between amplitudes $D_{l\pm1}$, $Q_{l,l\pm2}$ and $\breve{D}_{l\pm1}$, $\breve{Q}_{l,l\pm2}$, respectively.

To simplify the experimental detection of nondipole parameters, the cross section [Eq. (36)] has to be measured under so-called *magic angle* equal to $\vartheta_m = 57.3°$, for which $P_2(\cos \vartheta_m) = 0$, so that the contribution of the term with β_{nl} disappears. Under the angle ϑ_m the terms $\delta_{nl}^C(\omega)$ and $\gamma_{nl}^C(\omega)$ enter the cross section in the following combination:

$$\lambda_{nl}^C = \gamma_{nl}^C + 3\delta_{nl}^C. \qquad (46)$$

There are no data available on the quadrupole polarizabilities. This is why we have decided to omit both the dipole
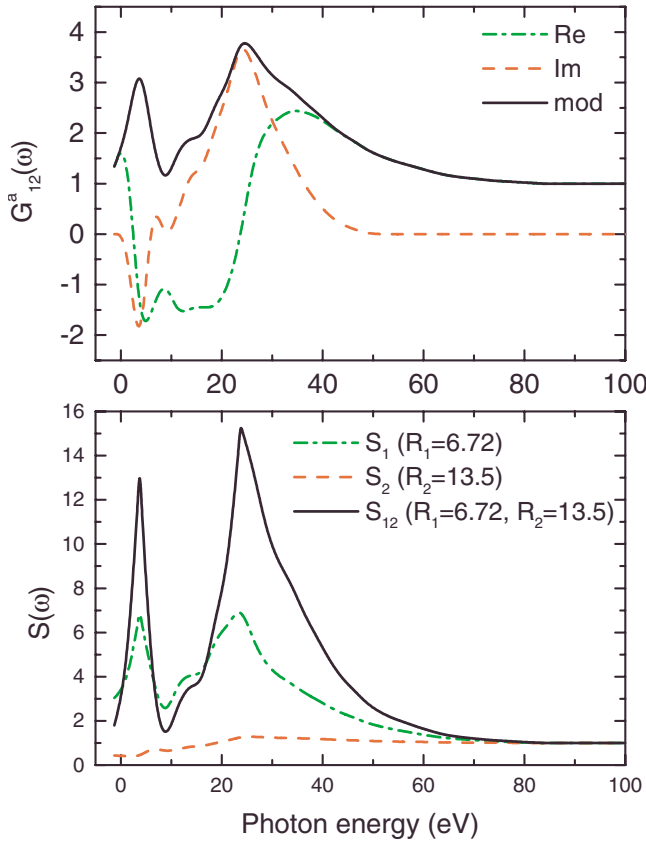
FIG. 1. (Color online) Polarization amplitude factor $G_{12}^a(\omega)$ (real, imaginary and absolute values) and polarization factors $S_1(\omega)$ for C_{60}, $S_2(\omega)$ for C_{240} and $S_{12}(\omega)$ for $C_{60}@C_{240}$.

and quadrupole polarization amplitude factors $G_{12}^d(\omega)$ and $G_{12}^q(\omega)$ in calculations of the nondipole parameters.

VII. RESULTS OF CALCULATIONS

As concrete objects of two-shell endohedral atoms we consider here $Ar@C_{60}@C_{240}$ and $Xe@C_{60}@C_{240}$ with the fullerenes parameters, presented in Sec. V. The following subshells are considered: $3p^6$ and $3s^2$ for Ar and $5p^6$, $5s^2$ and $4d^{10}$ for Xe. The results are presented in Figs. 1–11. They are obtained with the help of Eqs. (42)–(45) and similarly modified Eqs. (36)–(38) and (46). The results with account of reflection by a single fullerenes shell we denote on the figures as FRPAE, while results with two shells taken into account are marked as FRPAE2. Specially mentioned is the effect of polarization factor $\bar{G}_{12}(\omega)$. Since the reflection amplitudes $F_l(k)$ are different for different atoms, we are not presenting their values separately.

Figure 1 depicts the $\bar{G}_{12}(\omega)$ parameter from (31)—its absolute value, real and imaginary parts and shows the polarization factors $S_i(\omega) = |G_i(\omega)|$ separately for one shell or another and for two of them. The S factor for the big fullerene is small but its combination with the inner shell enhances the common S factor impressively. As it should be, effects of
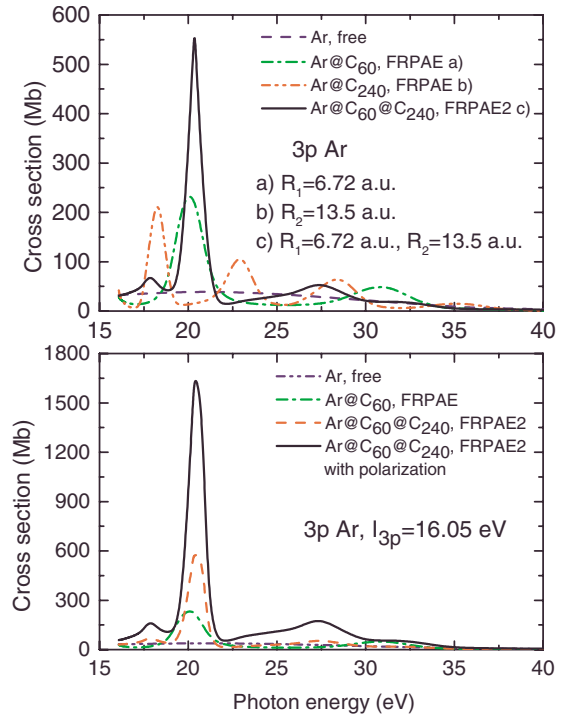

FIG. 2. (Color online) Photoionization cross-section of $3p$ electrons in Ar, $Ar@C_{60}$, $Ar@C_{60}@C_{240}$ with account of reflection factors F and for $Ar@C_{60}@C_{240}$ also with account of polarization factor $G_{12}^a(\omega)$.
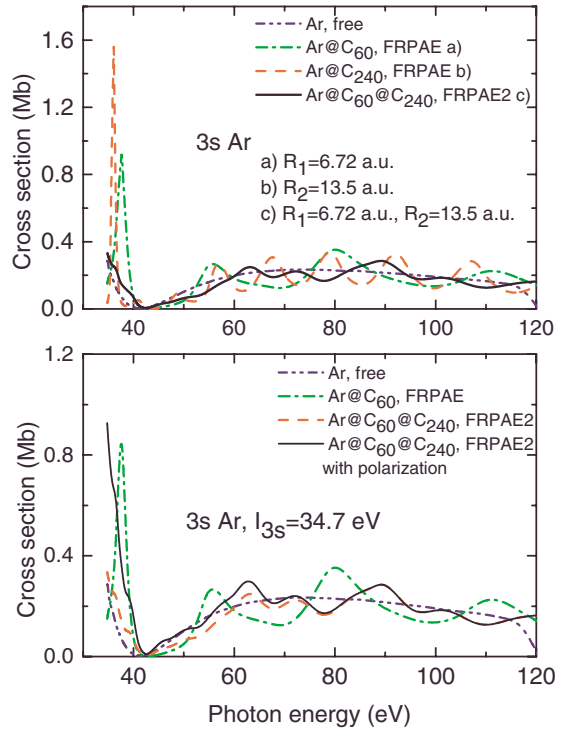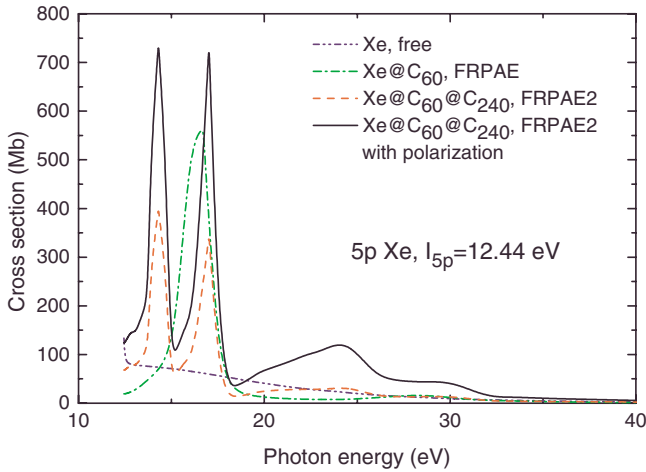

FIG. 3. (Color online) Photoionization cross-section of $3s$ electrons in Ar, $Ar@C_{60}$, $Ar@C_{240}$, and $Ar@C_{60}@C_{240}$ with account of reflection factors F and for $Ar@C_{60}@C_{240}$ also with account of polarization factor $G_{12}^a(\omega)$.

FIG. 4. (Color online) Photoionization cross section of $5p$ electrons in Xe, Xe@C_{60} and Xe@C_{60}@C_{240} with account of reflection factors F and the latter with account of polarization factor $G_{12}^a(\omega)$.

FIG. 6. (Color online) Photoionization cross section of $4d$ electrons in Xe, Xe@C_{60} and Xe@C_{60}@C_{240} with account of reflection factors F and the latter with account of polarization factor $G_{12}^a(\omega)$.

polarization are rapidly decreasing with ω growth, so that it approaches almost 1 at $\omega > 60$ eV.

Figure 2 presents the photoionization cross section for $3p$ in Ar, Ar@C_{60}, Ar@C_{240}, and Ar@C_{60}@C_{240}, i.e., with account of photoelectron scattering by one and two fullerenes shells. It is seen also profound action of the polarization factor G_{12}^a upon the Ar photoionization cross section. Note that two-shell reflection concentrates almost all cross section into a single maximum. This maximum is strongly enhanced by fullerenes shells polarization.

Figure 3 presents the same data as Fig. 2 but for photoionization of $3s$ Ar. The action of polarization upon $3s$ is prominent but mach smaller than upon $3p$. The effect of two-shell reflection even decreases the near threshold maximum.
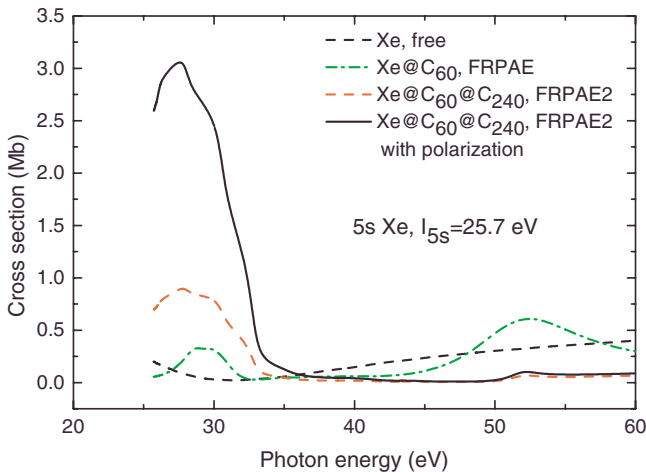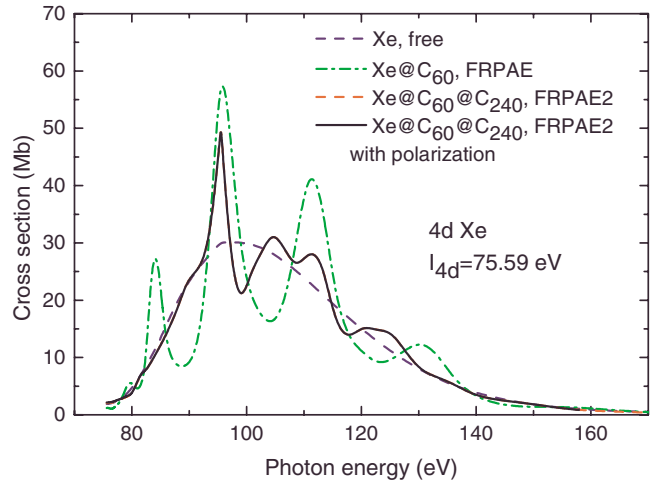
Figure 4 depicts photoionization cross section for $5p$ in Xe, Xe@C_{60}, Xe@C_{60}@C_{240} and demonstrates profound action of the polarization factor G_{12}^a upon the Xe $5p$ photoionization cross section. The effect of scattering by the second fullerenes shell is strong enough, presenting a distinctive
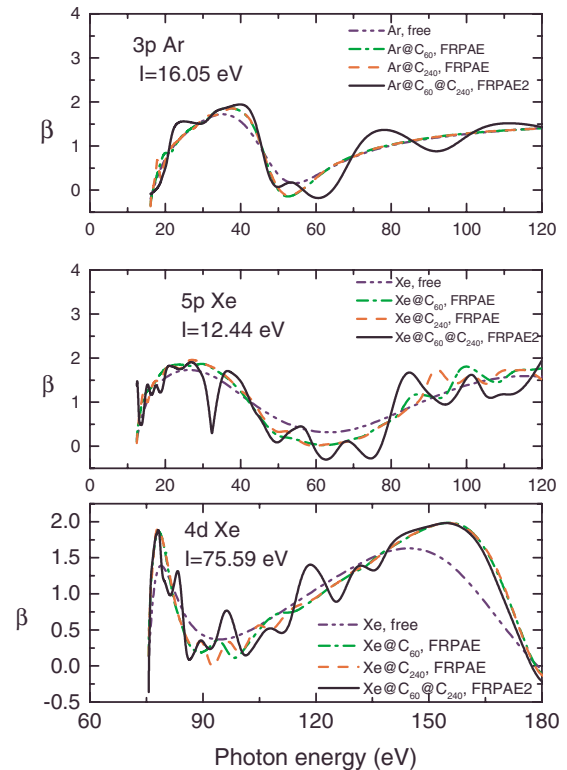

FIG. 7. (Color online) Dipole angular anisotropy parameter $\beta_{3p}(\omega)$ of $3p$ electrons in Ar, Ar@C_{60} and Ar@C_{60}@C_{240}, $\beta_{5p}(\omega)$ of $5p$ and $\beta_{4d}(\omega)$ of $4d$ electrons in Xe, Xe@C_{60}, Xe@C_{60}@C_{240} all with account of respective reflection factors F.

FIG. 5. (Color online) Photoionization cross section of $5s$ electrons in Xe, Xe@C_{60} and Xe@C_{60}@C_{240} with account of reflection factors F and the latter with account of polarization factor $G_{12}^a(\omega)$.
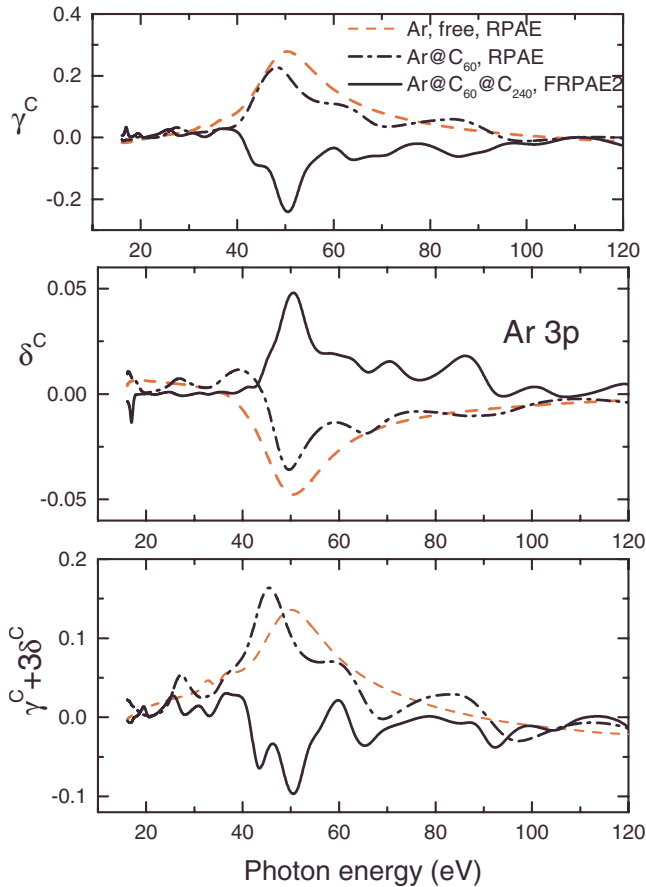
FIG. 8. (Color online) Nondipole angular anisotropy parameter $\gamma_{3p}^C(\omega)$, $\delta_{3p}^C(\omega)$ and their combination $\gamma_{3p}^C(\omega)+3\delta_{3p}^C(\omega)$ for 3p electrons in Ar, Ar@C$_{60}$ and Ar@C$_{60}$@C$_{240}$ with account of reflection factors F.

FIG. 9. (Color online) Nondipole angular anisotropy parameter $\gamma_{5p}^C(\omega)$, $\delta_{5p}^C(\omega)$ and their combination $\gamma_{3p}^C(\omega)+3\delta_{3p}^C(\omega)$ for 5p electrons in Xe, Xe@C$_{60}$ and Xe@C$_{60}$@C$_{240}$ with account of reflection factors F.

second maximum and decreasing the maximum that appear due to one-shell scattering. Polarization of fullerenes increases quite noticeable the cross section.

Figure 5 presents the same data as Fig. 8 but for photoionization of 5s in Xe. The role of polarization is strong at $\omega < 35$ eV.

Figure 6 depicts photoionization cross-section for 4d in Xe, Xe@C$_{60}$, Xe@C$_{60}$@C$_{240}$ and demonstrates action of the polarization factor G_{12}^a upon the Xe 4d photoionization cross section. Note that the role of polarization is very small and inclusion of two shells even suppresses the effect of only C$_{60}$.

Figure 7 demonstrates the angular anisotropy parameters $\beta_{3p}(\omega)$ of 3p electrons in Ar, Ar@C$_{60}$, Ar@C$_{60}$@C$_{240}$, $\beta_{5p}(\omega)$ of 5p and $\beta_{4d}(\omega)$ of 4d in Xe, Xe@C$_{60}$ and Xe@C$_{60}$@C$_{240}$ with account of reflection factors F. The effect of reflection is quite small, leading in Ar to a small oscillations around the photon energy region $\omega \approx 20$ eV. The effect in Xe is similar in size, but there are two regions of oscillations in 5p Xe instead of one in 3p Ar. For 4d the effect is stronger and is located in an area, where the relative effect is bigger.
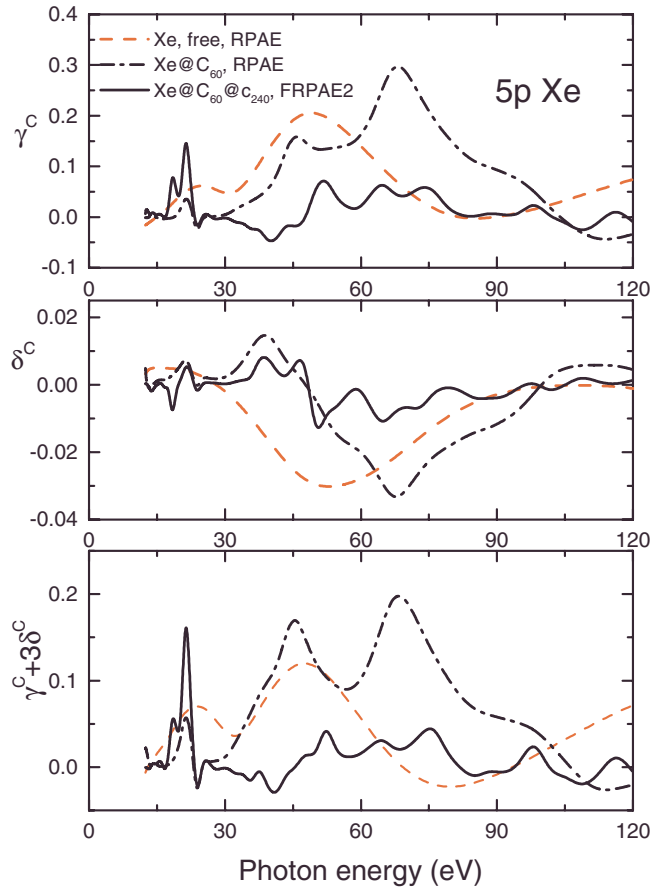
Figure 8 gives nondipole angular anisotropy parameters $\gamma_{3p}^C(\omega)$, $\delta_{3p}^C(\omega)$ and their combination $\gamma_{3p}^C(\omega)+3\delta_{3p}^C(\omega)$ for 3p electrons in Ar, Ar@C$_{60}$ and Ar@C$_{60}$@C$_{240}$ with account of reflection factors F. It is remarkable that while the C$_{60}$ shell adds only relatively small oscillations to $\gamma_{3p}^C(\omega)$ as compared to the value in an isolated atom, the additional C$_{240}$ shell leads to an almost complete "mirror reflection" of the respective free atom curve with noticeable oscillations on it. Qualitatively, the situation for $\delta_{3p}^C(\omega)$ is similar to that in $\gamma_{3p}^C(\omega)$, but the absolute values are by a factor of three smaller. For the combination of nondipole angular anisotropy parameters $\gamma_{3p}^C(\omega)+3\delta_{3p}^C(\omega)$ the inclusion of the second fullerenes shell apart of "mirror reflection" adds prominent structure to the curve.

Figure 9 depicts the nondipole angular anisotropy parameter $\gamma_{5p}^C(\omega)$, $\delta_{5p}^C(\omega)$, and their combination $\gamma_{3p}^C(\omega)+3\delta_{3p}^C(\omega)$ for 5p electrons in Xe, Xe@C$_{60}$ and Xe@C$_{60}$@C$_{240}$ with account of reflection factors F. While inclusion of the C$_{60}$ shell to some extend enhances the parameter $\gamma_{5p}^C(\omega)$, the second shell brings this parameter almost to zero except a noticeable maximum at $\omega \approx 20$ eV. The situation for $\delta_{5p}^C(\omega)$ is similar to that for $\gamma_{5p}^C(\omega)$. In Ar an outstanding feature in
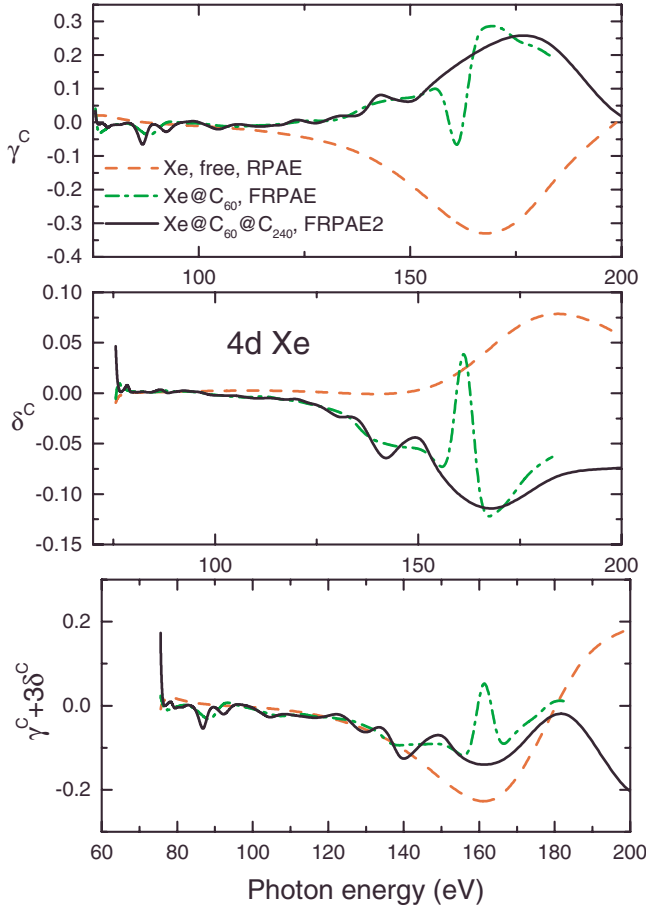
FIG. 10. (Color online) Nondipole angular anisotropy parameter $\gamma_{4d}^{C}(\omega)$, $\delta_{4d}^{C}(\omega)$ and their combination $\gamma_{4d}^{C}(\omega)+3\delta_{4d}^{C}(\omega)$ for $4d$ electrons in Xe, Xe@C$_{60}$ and Xe@C$_{60}$@C$_{240}$ with account of reflection factors F.
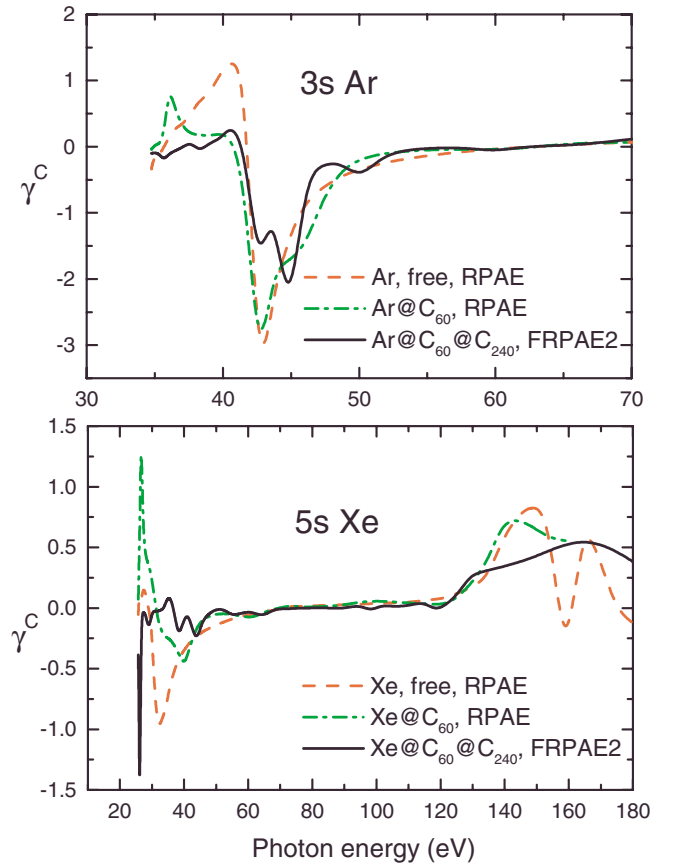

FIG. 11. (Color online) Nondipole angular anisotropy parameter $\gamma_{3s}^{C}(\omega)$ and $\gamma_{5s}^{C}(\omega)$ for $3s$ and $5s$ electrons in Ar, Ar@C$_{60}$, Ar@C$_{60}$@C$_{240}$ and Xe, Xe@C$_{60}$, Xe@C$_{60}$@C$_{240}$ with account of reflection factors F.

$\gamma_{3p}^{C}(\omega)+3\delta_{3p}^{C}(\omega)$ is a maximum at the same place as for $\gamma_{5p}^{C}(\omega)$.

Figure 10 demonstrates the nondipole angular anisotropy parameter $\gamma_{4d}^{C}(\omega)$, $\delta_{4d}^{C}(\omega)$, and their combination $\gamma_{4d}^{C}(\omega)+3\delta_{4d}^{C}(\omega)$ for $4d$ electrons in Xe, Xe@C$_{60}$, and Xe@C$_{60}$@C$_{240}$ with account of reflection factors F. The C$_{60}$ shell produces in $\gamma_{4d}^{C}(\omega)$ an oscillation at 150–175 eV, while the second fullerene shell makes the curve where it is non-zero an almost complete "mirror reflection" of the free atom curve. For $\delta_{4d}^{C}(\omega)$ already C$_{60}$ changes the sign of the parameter and ads an oscillation. The addition of C$_{240}$ brings again to a curve similar to "mirror reflection" of the isolated atom curve. For the combination of nondipole angular anisotropy parameters $\gamma_{4d}^{C}(\omega)+3\delta_{4d}^{C}(\omega)$ the modification due to two shells is most visible at $\omega>140$ eV, where the magnitude becomes smaller and at $\omega>180$ eV changes sign.

Figure 11 gives the nondipole angular anisotropy parameter $\gamma_{3s}^{C}(\omega)$ (a) and $\gamma_{5s}^{C}(\omega)$ (b) for $3s$ and $5s$ electrons in Ar, Ar@C$_{60}$, Ar@C$_{60}$@C$_{240}$ and Xe, Xe@C$_{60}$, Xe@C$_{60}$@C$_{240}$ with account of reflection factors F. The δ_{ns}^{C} parameter is equal to zero.

VIII. CONCLUSION

We present results for photoionization cross sections, dipole, and nondipole angular anisotropy parameters for outer in Ar and outer and intermediate in Xe subshells for endohedrals with two-shell fullerenes Ar@C$_{60}$@C$_{240}$ and Xe@C$_{60}$@C$_{240}$ and compare it to the respective data for isolated atoms. We have investigated effects of photoelectron scattering by two zero-thickness potential wells and modification of the incoming photon beam due to dipole polarization of both fullerenes shell.

A whole variety of resonances are found that obviously are far from being a simple sum of effects, given by single fullerenes shells. Particularly sensitive to the surrounding of fullerenes shell are nondipole angular anisotropy parameters. For them, however, the effect of deviation of real fullerenes shell potential from the ideal spherical shape [Eq. (1)] could be of importance.

We admit that the moment when investigation of photoionization of such objects as A@C$_{60}$@C$_{240}$ or similar will take place is not literally tomorrow. However, we hope to see them being performed in not too distant future. We believe that possible findings will justify the efforts.

[1] M. J. Puska and R. M. Nieminen, Phys. Rev. A **47**, 1181 (1993).

[2] G. Wendin and B. Wastberg, Phys. Rev. B **48**, 14764 (1993).

[3] L. S. Wang, J. M. Alford, Y. Chai, M. Diener, and R. E. Smalley, Z. Phys. D: At., Mol. Clusters, **26**, 297 (1993).

[4] P. Decleva, G. De Alti, and M. J. Stener, J. Phys. B. **32**, 4523 (1999).

[5] J.-P. Connerade, V. Dolmatov, and S. Manson, J. Phys. B **33**, 2279 (2000).

[6] M. Ya. Amusia, A. S. Baltenkov, and L. V. Chernysheva, JETP Lett. **87**, 200 (2008).

[7] M. Ya. Amusia and A. S. Baltenkov, Phys. Rev. A **73**, 062723 (2006).

[8] J.-P. Connerade and A. V. Solov'yov, J. Phys. B **38**, 807 (2005).

[9] A. Muller *et al.*, J. Phys.: Conf. Ser. **88**, 012038 2007.

[10] K. Mitsuke *et al.*, J. Chem. Phys. **122**, 064304 (2005).

[11] J. P. Lu and W. Yang, Phys. Rev. B **49**, 11421 (1994).

[12] L. Forró and L. Mihály, Rep. Prog. Phys. **64**, 649 (2001).

[13] M. Ya. Amusia, A. S. Baltenkov, and U. Becker, Phys. Rev. A **62**, 012701 (2000).

[14] M. Ya. Amusia, A. S. Baltenkov, and L. V. Chernysheva, Phys. Rev. A **75**, 043201 (2007).

[15] M. Ya. Amusia and A. S. Baltenkov, Phys. Lett. A **360**, 294 (2006).

[16] M. Ya. Amusia, A. S. Baltenkov, and B. G. Krakov, Phys. Lett. A **243**, 99 (1998).

[17] M. Ya. Amusia, *Atomic Photoeffect* (Plenum Press, New York, London, 1990).

[18] M. Ya. Amusia, Radiat. Phys. Chem. **70**, 237 (2004).

[19] J. Berkowitz, J. Chem. Phys. **111**, 1446 (1999).

[20] J. M. Cabrera-Trujillo, J. A. Alonso, M. P. Iñiguez, M. J. López, and A. Rubio, Phys. Rev. B **53**, 16059 (1996).

[21] M. Ya. Amusia and L. V. Chernysheva, Appl. Phys. **5**, 21 (2009) (in Russian).

[22] J. W. Cooper, Phys. Rev. A **42**, 6942 (1990); **45** 3362 (1992); **47**, 1841 (1993).

[23] A. Bechler and R. H. Pratt, Phys. Rev. A **42**, 6400 (1990).